ACS Macro Letters

Letter

pubs.acs.org/macroletters

Expandable Temperature-Responsive Polymeric Nanotubes

Shintaro Kawano and Marek W. Urban*

School of Polymers and High Performance Materials, Shelby F. Thames Polymer Science Research Center, The University of Southern Mississippi, Hattiesburg, Mississippi 39406, United States

Supporting Information

ABSTRACT: Materials with the ability of dimensional changes on demand exhibit many potential applications ranging from adaptive composites that mimic biological functions under extreme conditions to microfluidics or neural implants to stimulate components of the nervous systems. These studies show the synthesis of temperature-induced reversibly expandable nanotubes that were prepared by polymerization of *N*-isopropylacrylamide (NIPAAM) in the presence of biologically active 1,2-bis(tricosa-10,12-diynoyl)-*sn*-glycero-3-phosphocholine ($DC_{8,9}PC$) diacetylenic phospholipids (PL). As a result, thermally responsive poly-NIPAM-phospholipid nanotubes (PNNTs) were prepared. Polymerization reactions occur within hydrophilic regions of PL bilayers, whereas PL hydrophobic zones facilitate transport and supply of the monomer for polymerization. The unique feature of PNNTs is that, above 37 °C, the outer diameter (OD) as well as the wall thickness (WT) shrink by 20 and 55%, respectively, whereas the inner diameter (ID) increases by ~16%. This behavior is attributed to the PNIPAM backbone buckling induced by local rearrangements within PL bilayered morphologies. The presence of acetylenic moieties along the PL bilayers in PNNTs provides an opportunity for irreversible "locking" of designable dimensions, which is facilitated by the formation of cross-linked PNNTs (CL-PNNTs).

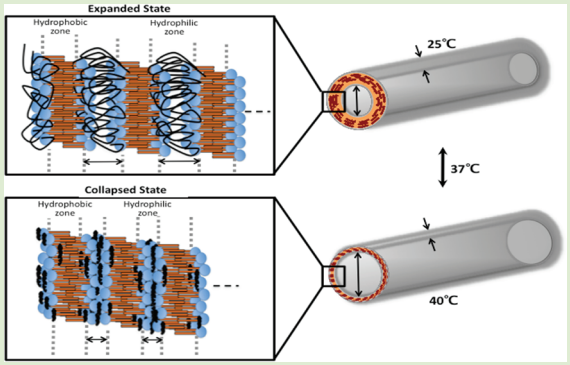

If functional objects that surround us had the ability of dimensional changes on-demand and to reversibly adopt by responding to environmental changes, new platforms of incredible technologies, ranging from reversible biomimetic actuators[1,2] to microfluidic devices[3] and neural implants,[4] or drug delivery systems[5] and physiologically diverted stents[6] can be envisioned. If designed properly, selected polymers meet some of these criteria,[7] but the main challenge is the shape design, its control, and fast dimensional reversibility. For example, colloidal hollow polymer particles,[8] polymerized lyposomes,[9,10] or other vesicles[11] have been prepared, which may exhibit temperature or pH responses, but directionally responsive tubular shapes are of particular interest for assembling more complex nanodevices with dimensional changes induced by a physiological temperature of ~37 °C.

This study reports the development of thermally responsive biocompatible nanotubes that were engineered by in situ assembly of biologically active phospholipids (PLs)[12] with simultaneous polymerization of *N*-isopropylacrylamide (NIPAM)[13] monomer that resulted in temperature-induced expandable poly-*N*-isopropylacrylamide-phospholipid nanotubes (PNNTs). Because these nanotubes are biocompatible and exhibit lower critical solution temperature (LCST) of 37 °C, they may find numerous applications in the biomedical field, thus, enabling dimensional changes under physiological conditions. Figure 1, A and B illustrates a two-step synthesis that results in the formation of PNNTs. In the first step, under redox conditions, potassium persulfate ($K_2S_2O_8^-$ KPS; oxidant) initiator and *N,N,N′,N′*-tetramethylethylenediamine ($C_6H_{16}N_2^-$ TEMED; reductant) were introduced into 1,2-bis(tricosa-10,12-diynoyl)-*sn*-glycero-3-phosphocholine ($DC_{8,9}PC$)[14] nanotubes (PLNT) dispersions. In the second step, in situ polymerization of NIPAM was conducted at room temperature, which resulted in PNNTs. Figure 1, A′ and B′ illustrates TEM images of PLNTs after each step and shows that upon polymerization inside and outside PLNT bilayers the wall thickness of PLNT changes from ~15 (A/A′) to 150 (B/B′) nm. Spectroscopic evidence that allowed us to determine PNNT chemical makeup is provided in the Supporting Information (Figures S1 and S2).

Dimensional responsiveness of PNNTs as a function of temperature is shown in Figure 2, A and B, which illustrate TEM images of PNNTs recorded at 25 and 40 °C. As seen, the most intriguing feature of PNNTs is shrinkage of the outside diameter (OD) from 660 nm at 25 °C to 530 nm at 40 °C, and an increase of the inside diameter (ID) from 370 to 430 nm, which is accompanied by wall thickness (WT) shrinkage from 142 to 67 nm. This is illustrated in the insets A′ and B′ of Figure 2. This behavior is attributed to the presence of polymerized PNIPAM inside and outside hydrophilic zones of PLNT interlayers. As shown in Figure 2, A′ and B′, the spacing between hydrophilic zones (white lines) changes from 29 nm at

Received: August 19, 2011
Accepted: December 21, 2011
Published: December 29, 2011

   dx.doi.org/10.1021/mz2000303 | *ACS Macro Lett.* 2012, 1, 232–235

Figure 1. Schematic diagram illustrating the formation process of PNNTs: step 1, self-assembly of DC8,9PC to PLNTs (A); step 2, PNNTs formed from free radical redox polymerization of NIPAM with KPS and TEMED as oxidant and reductant, respectively in PLNTs dispersions (B). TEM images of nanotubes after each step are illustrated in images A′ and B′, respectively.

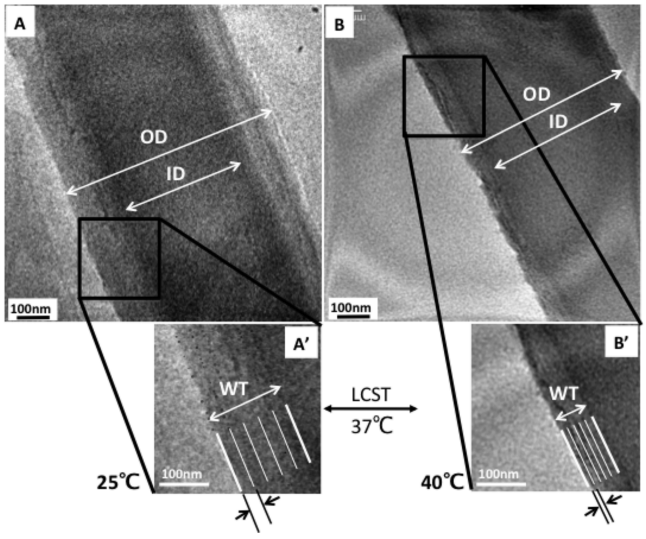

Figure 2. TEM images (A/B and A′/B′) of PNNTs prepared by redox polymerization of NIPAM in the presence of PLNT aqueous dispersion. The dispersions were cast on cupper grids and dried at 25 °C (A and A′) and 40 °C (B and B′). Images A′/B′ also illustrate PNIPAM interlayers between hydrophobic zones of PLs (parallel solid lines).

25 °C to 13 nm at 40 °C. These data also show that PNIPAM primarily resides within hydrophilic interlayers of PLNTs, thus, suggesting that NIPAM monomers diffuse into PLNTs interlayers to polymerize. Although it is anticipated that KPS polymerization initiator diffuses and resides in the hydrophilic $N^+(CH_2)_2PO_4^-$ parts of PL bilayers, hydrophobic zones of PL bilayers retain their structural features during polymerization and acetylenic C≡C entities retain their state, as manifested by spectroscopic evidence provided in Figure S3, trace A. However, exposure to UV radiation (304 nm) for 30 min results in the formation of C═C/C≡C conjugates, as shown in trace B of Figure S3. As a result, cross-linked PNNTs (CL-PNNTs) are formed. Attributed to the cross-linked PL interlayers that immobilize trapped PNIPAM, CL-PNNTs do not exhibit dimensional changes as a function of temperature, which is illustrated by TEM images in Figure S4. These observations also show that hydrophilic PL interlayers serve as polymerization *loci*, whereas hydrophobic PL bilayers allow transport of the monomer to the reaction sites.

To elucidate molecular origins of the dimensional changes in PNNTs as a function of temperature, Raman analysis was performed. While details pertaining to the spectroscopic data analysis are provided in Supp. Doc. (Figure S6), Figure 3 illustrates Raman spectra of PNNTs as a function of temperature. The main temperature-induced spectral features, the bands at 1137 and 1268 cm^{-1} due to C−C isopropyl and amide III (C−C−N; coupling between amide and isopropyl) increase at elevated temperatures. These observations are attributed to strong intramolecular interactions of isopropyl chains of PNIPAM, indicating that the formation of PNIPAM globular structures occurs upon cleavage of H-bonding interactions between PL bilayers and PNIPAM within the PL hydrophilic zone. At the same time, the band at 1457 cm^{-1} (isopropyl C−H asymmetrical deformation) decreases, indicating that isopropyl CH_3 segments of globular PNIPAM interact with PL bilayers aliphatic chains. These conclusions are supported by the fact that the Raman active bands in the 400−750 cm^{-1} region (not shown) due to PO_4^- and CN^+ entities in PNNTs are not affected by temperature, implying that the head $N^+(CH_2)_2PO_4^-$ PL groups do not participate in molecular rearrangements during PNIPAM shrinkage and expansion. Parallel ATR FT-IR analysis (Figure S6) supports these data and shows that, at 25 °C, PNIPAM interacts with acyl C═O groups of PL bilayers and residual water molecules. At 40 °C, the amide I band intensity decreases, whereas the amide II bands shifts to higher wavenumber, thus indicating that above LCST the coil-to-globule transitions occurs. These observations are consistent with temperature studies on neat PNIPAM.

To correlate molecular rearrangements responsible for dimensional changes of PNNTs with coil-to-globule transitions observed in PNIPAM,[15−17] thermal analysis was performed. Thermal transitions detected for PNIPAM solutions and PNNTs dispersions occur at 32 and 37 °C (Figure S7; heating rate of 0.5 °C/min), respectively, and represent LCST.[15] The increase of the LCST in PNNTs is attributed to acyl interactions with amide groups of PNIPAM and water within constrained hydrophilic interlayers,[18] thus supporting spectroscopic analysis.

Figure 4 summarizes temperature response of PNNTs below (25 °C) and above (40 °C). Below LCST (25 °C), hydrophobic PL zones retain their integrity, whereas PNIPAM hydrophilic zones are in their expended state. Above LCST (37 °C) at 40 °C, PNIPAM macromolecules within the hydrophilic PL interlayers collapse due to the coil-globular transitions, thus resulting in intra chain molecular arrangements within PNIPAM isopropyl chains manifested by internalized adsorption of PNIPAM onto hydrophobic parts of PL bilayers. This results in decreased OD and WT of PNNTs. While hydrophilic interlayers shrunk at 37 °C, hydrophobic zones exhibit amorphous "accordion-like" behavior due to formation of a ripple phase between solid and liquid crystal-like phases of PL bilayers,[19] thus, increasing the strain and aiding to the dimensional changes of WT above the LCST.

dx.doi.org/10.1021/mz2000303 | *ACS Macro Lett.* 2012, 1, 232−235

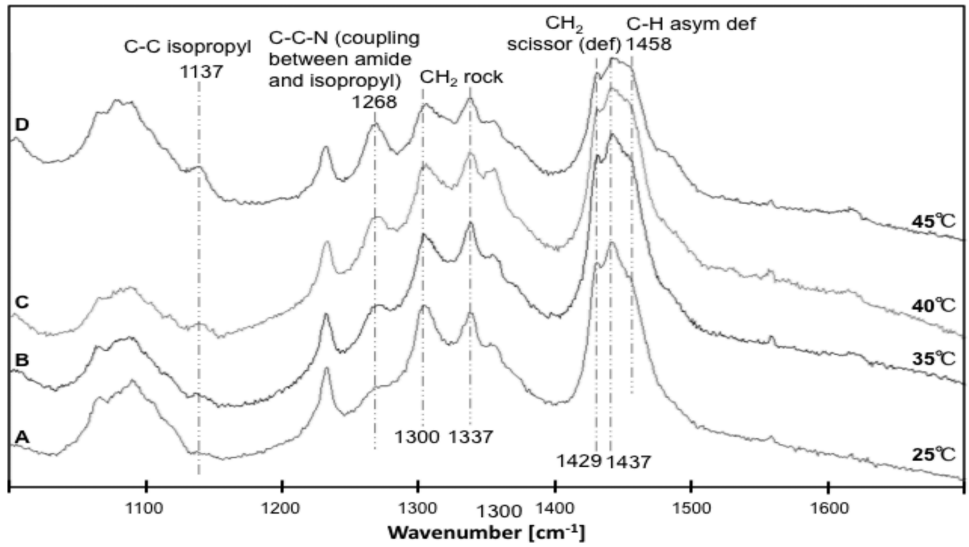

Figure 3. FT-Raman spectra in the 1000−1700 cm^{-1} region of PNNT recorded as a function of temperature at 25 (A), 35 (B), 40 (C), and 45 °C (D).

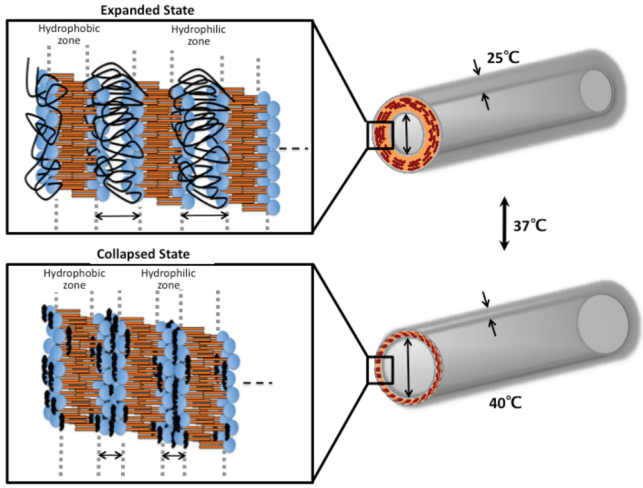

Figure 4. Schematic diagram of temperature-sensitive PNNTs.

Preparation of polymeric nanotubes: In a typical procedure, 1,2-bis(10,12-tricosadiynoyl)-*sn*-glycero-3-phosphocholine ($DC_{8,9}PC$) nanotubes (PLNTs) were obtained using the literature method (see methods for PLNT preparation). A total of 5 mL of an aqueous dispersion with 2.2 mM PLNTs and 22 mM NIPAM was purged with N_2 for 0.5 h, followed by the addition of 1 mL of 6.3 mM KPS aqueous solution, which served as an oxidant agent. After 10 min, the final step involved the addition of 13 mM of TEMED, which acted as a reducing agent to react with the oxidant agent. The reaction continued for 2 h, after which the product was collected by centrifugation to remove excess ions, unreacted monomer and free PNIPAM.

Preparation of phospholipid nanotubes: 1,2-bis(10,12-tricosadiynoyl)-*sn*-glycero-3-phosphocholine ($DC_{8,9}PC$) was purchased from Avanti Polar Lipids, Inc. $DC_{8,9}PC$ nanotubes (PLNTs) were obtained using the literature method.[20] In a typical synthesis, the following process was followed. A 10 mg aliquot of $DC_{8,9}PC$ was added into 10 mL of ethanol/water (7:3 v/v) solution, followed by allowing to equilibrate in water bath at 60 °C for 1 h. The solution was cooled at at room temperature for 1 h and then kept in refrigerator overnight. The dispersion was centrifuged at 3000 rpm followed by rinsing several times in deionized (DI) water.

Preparation of thermoresponsive polymeric nanotubes: *N*-isopropylacrylamide (NIPAM), potassium persulfate (KPS; $K_2S_2O_8$), and *N*,*N*,*N*′,*N*′-tetramethylethylenediamine (TEMED) were purchased from Aldrich Chemical Co. A schematic diagram illustrating the formation of poly(*N*-isopropylacrylamide) (PNIPAM) $DC_{8,9}PC$ nanotubes (PNNTs) is shown in Figure 1. A total of 5 mL of an aqueous dispersion with 2.2 mM PLNTs and 22 mM NIPAM was purged with N_2 for 0.5 h, followed by the addition of 1 mL of 6.3 mM KPS aqueous solution, which served as a oxidant agent. After 10 min, the final step involved the addition of 13 mM of TEMED, which acted as a reducing agent to react with the oxidant agent. The reaction continued for 2 h, after which the product was collected by centrifugation to remove excess ions, unreacted monomer, and free PNIPAM. To cross-link diacetylene groups of $DC_{8,9}PC$ to C═C/C≡C conjugated interlayer, UV irradiation was used for 30 min at room temperature using a fluorescent UV lamp with an UV output of 120 W and maximum emission at 301 nm. The distance between the lamp and the sample dispersion was 8 cm. The dispersion solution was stirred magnetically to ensure a homogeneous irradiation.

Characterization of morphological and spectroscopic features of polymeric nanotubes: Morphological features as a function of temperature were analyzed using a JEOL JEM-2100 transmission electron microscope (TEM) operated at 200 kV, in which samples were diluted and deposited on Formvar/carbon-coated copper grids. Upon PNNT deposition on a grid, each specimen maintained their temperature by placing it in an oven set at 25 or 40 °C. Proton NMR spectra were acquired using a Varian Mercury 300 MHz NMR spectrometer. Typical measurement conditions involved a 45° pulse, relaxation delay of 1 s, and an acquisition time of 1.998 s. Each spectrum represents the coaddition of 32 scans. For each measurement, 1 wt % of PNNTs was dissolved in deuterated chloroform (CD_3Cl). Microscopic attenuated total reflectance Fourier transform infrared (ATR-FT-IR) spectra were collected on a Bio-Rad FTS-6000 FT-IR single-beam spectrometer set at 4 cm^{-1} resolution equipped with a deuterated triglycine sulfate

dx.doi.org/10.1021/mz2000303 | *ACS Macro Lett.* 2012, 1, 232−235

(DTGS) detector. A 2 mm Ge crystal with a 45° face angle maintaining constant contact pressure between the crystal and the specimens was used. An amount of 10 μL of dispersion was placed directly on the Ge crystal and allowed to dry at least 1 h to form a layer of film on the crystal, followed by N_2 purging for 30 min. To study the thermosensitive properties, each spectrum of the film surface was measured on the Ge crystal with attached heating controller (Pike technology; Omega CN800 thermo controller) after each sample was equilibrated at a given temperature for 30 min. Spectra represented 100 coadded scans rationed to 100 scans collected on an empty ATR cell. All spectra were corrected for spectral distortions by Q-ATR software using the Urban-Huang algorithm.[21] Fourier transform Raman (FT-Raman) spectra were obtained with a Renishaw inVia Raman microscope equipped with a computer-controlled three-axis encoded (XYZ) motorized stage, a RenCam CCD detector, and a Leica microscope (DMLM series). The 520 nm diode laser provided Raman excitation with a maximum power output of 300 mW. The sample solutions were deposited on the gold substrate and allowed to dry. The Raman spectra of samples were collected with a 30 mW laser power on the sample and an acquisition time of 50 s. In examination of the thermosensitive properties, each spectrum was measured with the samples, which were prepared by drying of the dispersions on the gold substrates and allowing to stay on an attached heating stage to dry at room temperature and at consequently elevated temperatures (30, 35, 40, and 45 °C). Differential scanning calorimetry (DSC) measurements were performed on a TA Instruments DSC Q100 under a N_2 atmosphere. DSC thermal cycles were conducted using the following conditions: sample solutions were equilibrated at 10 °C for 5 min, followed by heating at 0.5 °C/min to 40 °C (or 5 °C/min to 70 °C), equilibrating at 40 °C (or 70 °C) for 5 min, and cooling down at 5 °C/min to 10 °C. The resulting data were analyzed using TA Universal Analysis software.

■ ASSOCIATED CONTENT

Supporting Information

Additional experimental details and supporting figures. This material is available free of charge via the Internet at http://pubs.acs.org.

■ AUTHOR INFORMATION

Corresponding Author

*E-mail: marek.urban@usm.edu.

Notes

The authors declare no competing financial interest.

■ ACKNOWLEDGMENTS

Research Fellowship Program of the Japan Society for the Promotion of Science for Young Scientists is acknowledged (S.K.). The authors also acknowledge the use of shared facilities through the Materials Research Facilities Network (MRFN) supported by the NSF MRSEC program (DMR 0213883) as well as Major Research Instrumentation program DMR 0215873.

■ REFERENCES

(1) Osada, Y.; Okuzaki, H.; Hori, H. *Nature* **1992**, *355*, 242−244.
(2) Jager, W. H. E.; Smela, E.; Ingana, O. *Science* **2000**, *290*, 1540−1545.
(3) Goldberger, J.; Fan, R.; Yang, P. *Acc. Chem. Res.* **2006**, *39*, 239−248.
(4) Stieglitz, T. *J. Neural. Eng.* **2009**, *6*, 1−11.
(5) Langer, R. *Nature* **1998**, *392*, 5−10.
(6) Lendlein, A.; Langer, R. *Science* **2002**, *296*, 1673−1676.
(7) Stuart, M. A. C.; Huck, W. T. S.; Genzer, J.; Müller, M.; Ober, C.; Stamm, M.; Sukhorukov, G. B.; Szleifer, I.; Tsukruk, V. V.; Urban, M.; Winnik, F.; Zauscher, S.; Luzino, I.; Minko, S. *Nat. Mater.* **2010**, *9*, 101−113.
(8) Lestage, D. J.; Urban, M. W. *Langmuir* **2005**, *21*, 4266−4267.
(9) Bellomo, E. G.; Wyrsta, M. D.; Pakstis, L.; Pochan, D. J.; Deming, T. J. *Nat. Mater.* **2004**, *3*, 244−248.
(10) Li, M.-H.; Keller, P. *Soft Matter* **2009**, *5*, 927−937.
(11) Kono, K. *Adv. Drug Delivery Rev.* **2001**, *53*, 307−319.
(12) Schnur, J. M. *Science* **1993**, *262*, 1669−1676.
(13) Heskins, M.; Guillet, J. E. *J. Macromol. Sci.* **1968**, *2*, 1441−1455.
(14) Yager, P.; Schoen, P. E. *Mol. Cryst. Liq. Cryst.* **1984**, *106*, 371−381.
(15) Liu, F.; Jarrett, W. L.; Urban, M. W. *Macromolecules* **2010**, *43*, 5330−5337.
(16) Katsumoto, Y.; Tanaka, T.; Sato, H.; Ozaki, Y. *J. Phys. Chem. A* **2002**, *106*, 3429−3435.
(17) Maeda, Y.; Higuchi, T.; Ikeda, I. *Langmuir* **2000**, *16*, 7503−7509.
(18) Bergbreiter, D. E.; Case, B. L.; Liu, Y.-S.; Caraway, J.W. *Macromolecules* **1998**, *31*, 6053−6062.
(19) Mueller, A.; O'Brien, D. F. *Chem. Rev.* **2002**, *102*, 727−757.
(20) Georger, J. H.; Singh, A.; Price, R. R.; Schnur, J. M.; Yager, P.; Schoen, P. E. *J. Am. Chem. Soc.* **1987**, *109*, 6169−6175.
(21) Urban, M. W. *Attenuated total reflectance spectroscopy of polymers; Theory and applications*; American Chemical Society and Oxford University Press: Washington, DC, 1996.